Laser welded reactor fuel element prototype

Laser Welding of a Simulated Nuclear Reactor Fuel Assembly

Study develops parameters for pulsed ruby laser welding, reports improvement of earlier cracking problems but does not meet penetration requirements

BY C. L. ESTES AND P. W. TURNER

ABSTRACT. A pulsed ruby laser was evaluated for welding a simulated nuclear reactor fuel pin bundle to a tube sheet. Tube-to-tube sheet welds joined AISI 304 tube sheets to AISI 316 tubular assemblies which were arranged in a unique, close-packed configuration causing the joints to be inaccessible for joining by conventional welding processes. The electron beam process was also evaluated and was eventually selected instead of the laser process, for fabricating experimental tube bundles.

C. L. ESTES was Development Engineer (now retired) and P. W. TURNER is Welding Laboratory Supervisor, Development Division, Union Carbide Corporation Nuclear Division, Oak Ridge, Tennessee.

This choice was justified because a subsequent change in joint efficiency (deeper penetration) made it impractical to use the existing laser welding machine. A detailed coverage of the development of the electron beam welding procedure is not presented because it is not within the scope of this paper.

Introduction

As part of a development program an internally heated test assembly was designed to simulate a subsize nuclear power reactor fuel subassembly. It consisted of a header (tube sheet) made of AISI 304 stainless steel and a cluster of nineteen 0.230 in. OD AISI 316 stainless steel tubes. Each of these tubes was the sheath of a commercial electric cartridge heater composed of a Nichrome heating element brazed to a 0.140 in. diam copper rod which conducted electrical energy into the 48 in. long heater. A copper conductor was swaged into each tube. A layer of boron nitride was placed between the heating element and the inner surface of the tube before swaging, and a mica plug was used as an insulator-sealant at the open end of the unit. The purpose of this assembly was to provide controlled heating of liquid sodium during experimental testing.

The original design of the mockup specified a minimum extension of the copper rods above the header of 2.600 in. Specifications for seal welding tubes to tube sheets included a minimum of 0.012 in. penetration and no detectable helium leak at a mass spectrometer sensitivity of 1.0×10^{-9} std cc/sec.
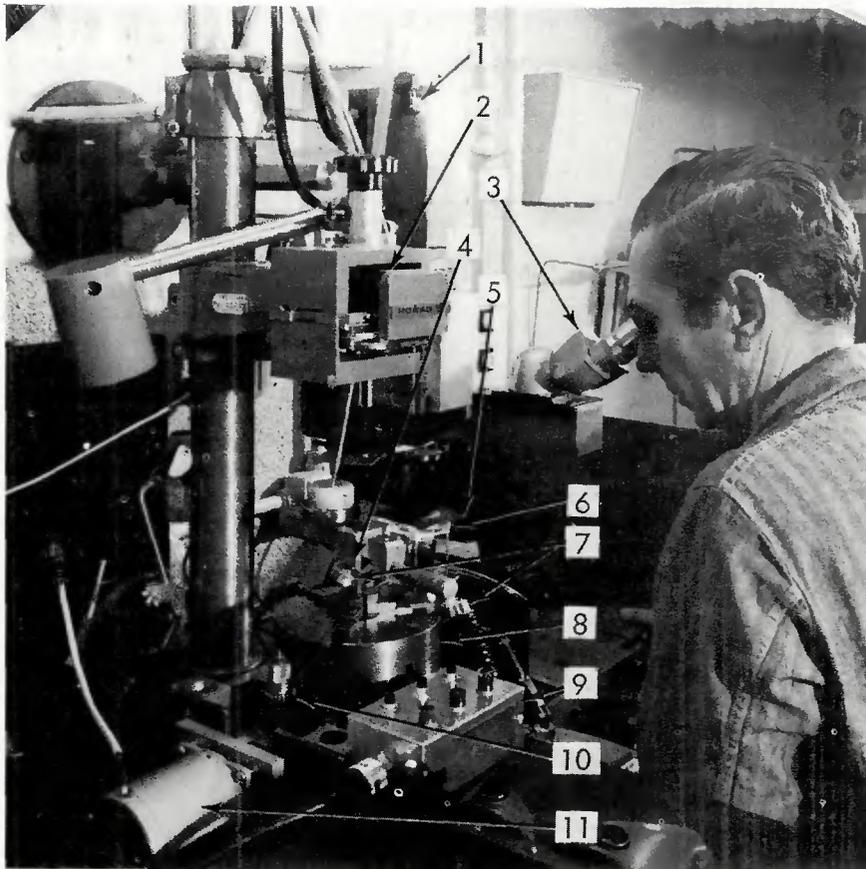
Fig. 1 — Laser welding station and tooling for making circular (tube-to-header) welds automatically: (1) laser cavity, (2) rotating mechanism, (3) viewing optics, (4) weld diameter adjustment, (5) mirror, (6) purge box, (7) lights, (8) chuck, (9) remote controls, (10) clutch, and (11) indexing motor
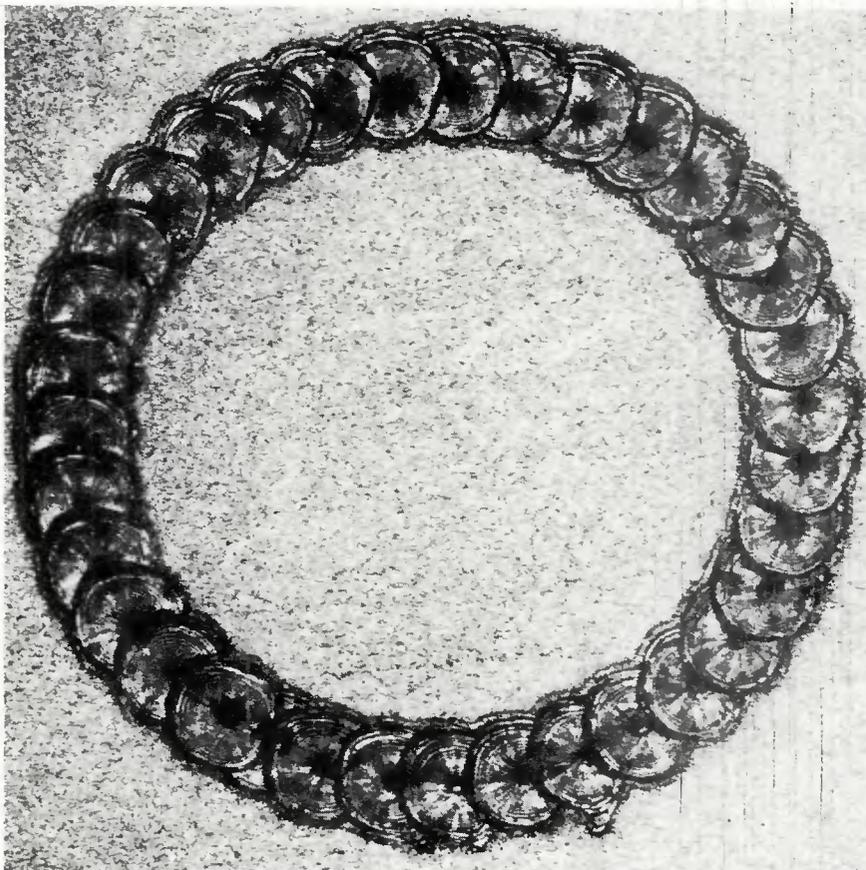

Fig. 2 — Circular laser weld consisting of a series of overlapping spot welds (X19)

Because the nineteen welds with protruding copper rods were closely packed within a 1.250 in. diam circular area, precise control was required to direct heat into the areas to be joined. The array of nineteen tubes is shown at the center of the lead photograph. Design and service requirements precluded the use of brazing. These limitations narrowed the field of applicable joining processes to electron beam and laser welding. An electron beam machine with chamber capacity that would accommodate the 5 ft long assembly and precision tooling for positioning and rotating the unit were not available during this phase of the program. However, previous work on edge joints (Ref. 1) indicated that the laser welding process was a candidate for welding the mockup; therefore, a program was initiated to determine the feasibility of welding the assembly with existing pulsed ruby laser welding equipment.

Equipment and Tooling

A pulsed ruby laser welding machine rated at 10 joules per pulse at a pulse repetition rate of 30 pulses per minute (continuous duty cycle) and a pulse time of 1 to 5 milliseconds was used for this study.

The laser welding station equipped with controls and tooling for making circular welds like those illustrated in the lead photograph is shown in Fig. 1. The rod attached to the laser head rotating mechanism (2), which was designed for hand manipulation, was connected to a weld diameter adjusting slide (4). This slide is mounted in a chuck (8) driven by a stepping motor (11) that is preset by indexing controls (not shown). A signal from the pulse repetition timer actuates the stepping motor after each pulse, and the welding head is moved forward a preset distance around the fixed circular weld. The indexing amplitude is adjustable for control of spot overlap. A clutch (10) is provided for manually rotating the laser head during setup and alignment.

A mirror (5) having a 0.750 in. diam hole for passage of the laser beam was mounted on the lower lens housing. Opposing lights (7) were directed toward the mirror which reflected uniform lighting around the copper pins. The workpiece can be positioned and aligned by means of a hand-operated cross slide which supports the workpiece. A purge box (6), fabricated from 0.125 in. thick distortion-free Pyrex through which the laser beam passed, was used to contain an argon atmosphere around the weldment.

Figure 2 shows a circular weld consisting of a series of overlapping spots that was made with the automatic setup to check the precision of

the positioner. Tooling for making linear welds automatically is also included in the welding station.

Control of Variables

Four process variables considered important to the success of this welding effort were charging voltage, pulse time, energy output, and the temperature of the cooling water. Therefore, the range of these variables was determined for a specific control setting. Then the results of variations on penetration and leak rate were evaluated.

Monitoring Four Variables

A multichannel recording oscillograph was used for monitoring the four variables. A silicon diode installed in the cooling water return line from the laser cavity provided a signal for monitoring the cooling water temperature in a range of 60 to 80 F. A beam splitter sampling technique was employed to provide signals for monitoring the laser pulse energy and pulse width (Ref. 2). A precision voltage divider attached to the charging voltage output terminals provided a signal for monitoring the laser charging voltage.

The cooling water monitor indicated that water temperature could be controlled within a 10 F range for a welding schedule of 125 consecutive pulses at 30 pulses per minute and energy output of 10 joules per pulse.

No measurable difference in penetration or leak rate that could be attributed to change in water temperature was noted over this range. Pulse time was within the manufacturer's 1 to 5 millisecond rating. Recorded charging voltage correlated well with the reading of the welder voltmeter. The energy output monitor provided reproducible indications of the laser output energy. A variation of 1/4 joule at 10 joules per pulse output was indicated.

Variation of Focal Distance

Figure 3 shows schematically the laser and viewing optical paths of the laser welding equipment. It is presented to show the relationship of the lower achromatic lens (movable) to the upper achromatic lens (fixed) and to the workpiece. The distance between the two lenses, within which the beam is collimated, is determined by limits designed to restrict the vertical movement of the lens housing, which contains the lower lens, to a maximum of two inches. The correct distance between the lower lens and the workpiece is a function of the focal length of the lens being used and will be referred to as focal dis-

tance in this paper. Normally, it is adjusted by observing the workpiece surface through the viewing optics and raising or lowering the lower lens until best visibility of the workpiece surface is obtained (sharp focus). The focal distance is an important variable having a strong influence on depth of penetration. Changes in penetration are often traceable to the variation in visual acuity of laser operators.

The graph in Fig. 4 shows the results of an experiment designed to relate focal distance to penetration. Spot welds were made on a section of 0.016 in. thick AISI 316 stainless steel. A spot made with the beam focused sharply on the surface of the sheet penetrated 0.007 in. into the coupon. After micrometer measurements of focal distance at sharp focus

were taken, the distance was increased in increments of 0.010 in. and a spot was made at each setting at plus 0.010 through plus 0.040 in. The focal distance was then decreased in the same manner back to sharp focus to verify the repeatability of the equipment. As may be noted, a 0.010 in. increase in focal distance
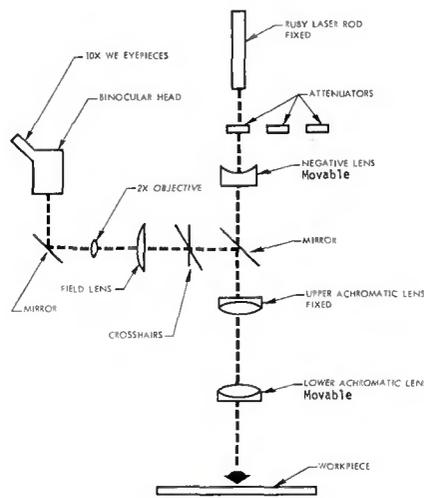

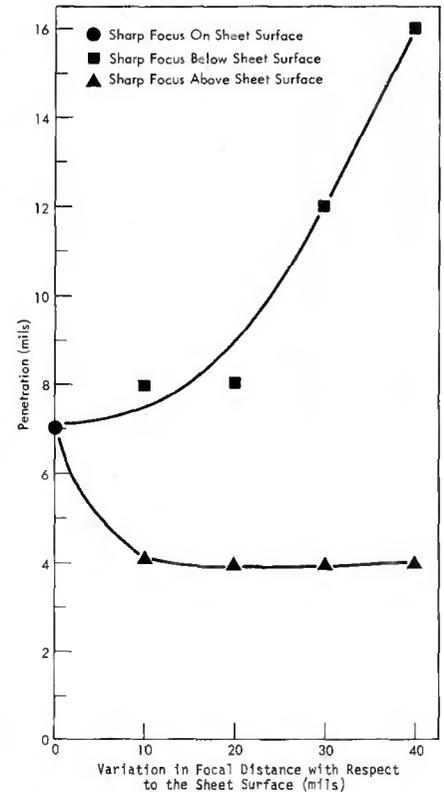Fig. 4 — Effect of focal distance on penetration of laser welds on 0.016 in. thick AISI 304 sheet
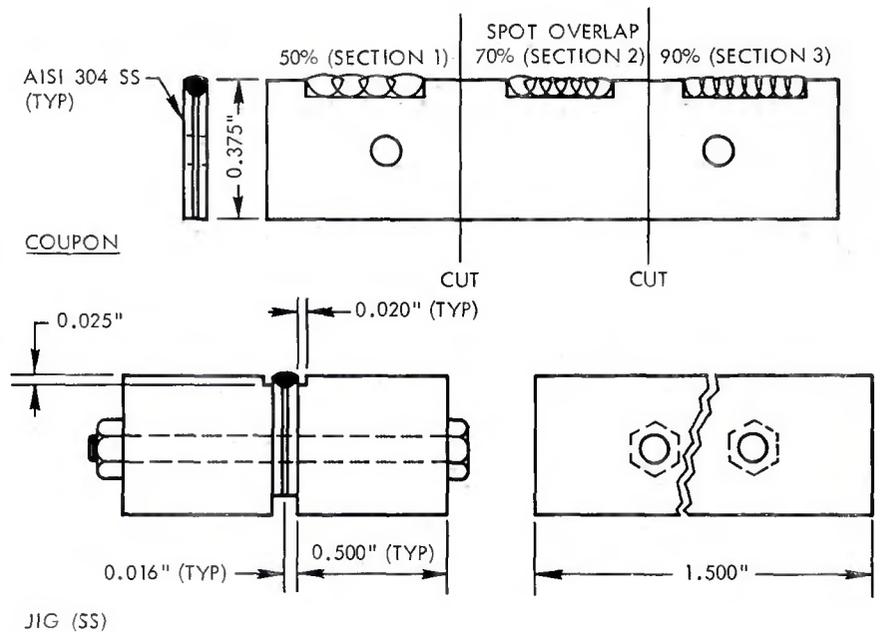

Fig. 3 — Laser optics

Fig. 5 — Spot overlap, laser weld test coupon and welding jig

resulted in approximately 50% reduction in penetration, and at greater increases, penetration remained substantially constant over the entire plus range. On the other hand a remarkable increase in penetration occurred when the focal distance was decreased by adjusting the location of sharp focus to positions below the sheet surface.

Variation of Spot Overlap

The relationship of spot overlap to penetration in pulsed laser welds is of special interest and is an important variable when maximum penetration capability of the pulsed laser beam is desired. Figure 5 shows a weld penetration test coupon and welding fixture. The coupon consisted of two sections of AISI 316 stainless steel 0.016 in. thick. The coupon sections were clamped in the fixture to form an edge joint which simulated the trepanned fuel failure mockup joints. Identical parameters were used to weld three areas on the coupons at 50, 70, and 90% spot overlap.

After welding, the coupon was sectioned as shown. The sections were mounted for metallographic processing with a flat side uppermost, and an attempt was made to polish through one 0.016 in. thick section to obtain a penetration profile along the longitudinal direction of the weld. After processing in this plane, coupons were demounted and remounted so that a cross-sectional view transverse to the weld was presented for metallography. Figure 6 shows longitudinal and transverse views of the weld made with 50% spot overlap. Welds made with 70 and 90% overlapping spots are shown for comparison.

Based on these data a compromise between a smooth weld bead surface and effective penetration is indicated. Although additional work to further optimize spot overlap was performed, 70 to 75% overlap was selected for welding the fuel mockup.

Pre-Mock Feasibility Study

Initially, short tubes machined from AISI 316 wrought bars were welded into subsized coupons. Seven welds were arranged to represent the center and inner circle of holes in the fuel mockup. The joint geometry of the simulated heater assembly is detailed in Fig. 7. Table 1 shows the leak rate and penetration resulting from various changes in parameters for the series of seven welds. Figure 8 illustrates Coupon 1 with copper rods removed to reveal weld appearances. Weld 2 has 0.001 to 0.002 in. depressions between spots which resulted from insufficient spot overlap (50%) to produce a smooth surface. In Fig. 9

cross sections of Welds 2 and 5 are shown to indicate the absence of cracks and porosity which later plagued the welding of the mockup.

The significance in the relationship

between charging voltage, the source of power output, and spot overlap becomes apparent by comparing the cross sections. A voltage of 3.60 kV and 50% overlap provided about the

70-0059-9   Longitudinal

70-0080-4   Transverse

70-0052-5   Longitudinal

70-0080-2   Transverse

70-0052-3   Longitudinal
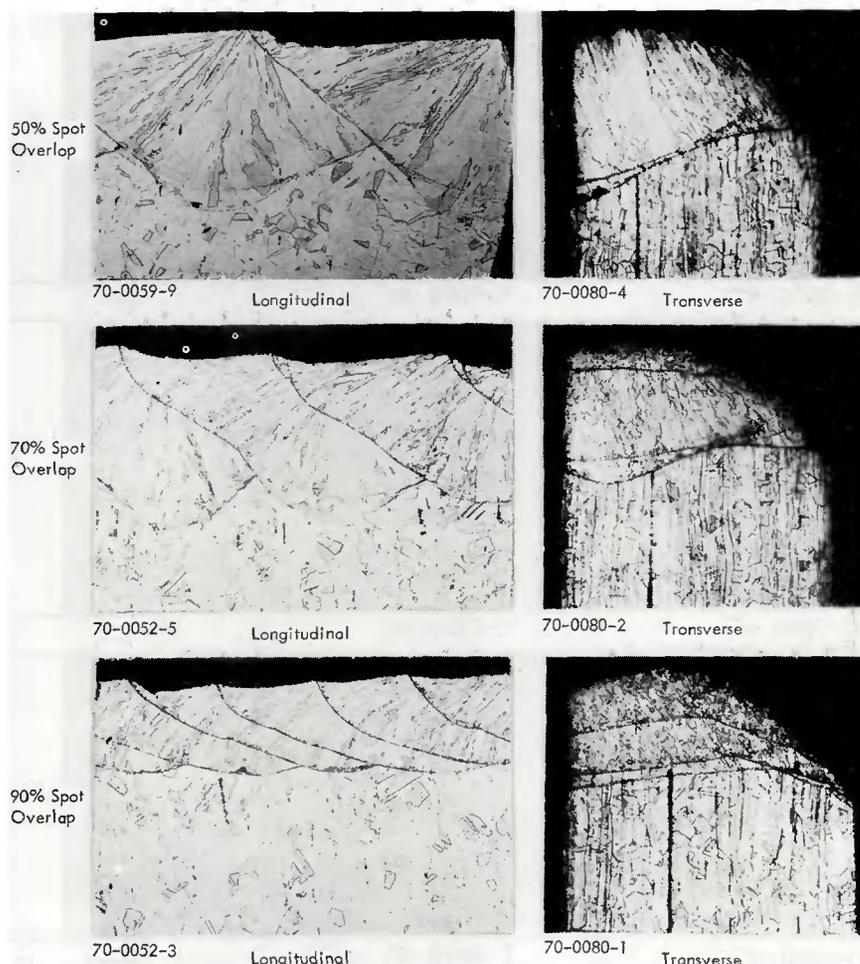
70-0080-1   Transverse

Fig. 6 — Mutually perpendicular views of laser welds with 50, 70, and 90% spot weld overlap, (X57)
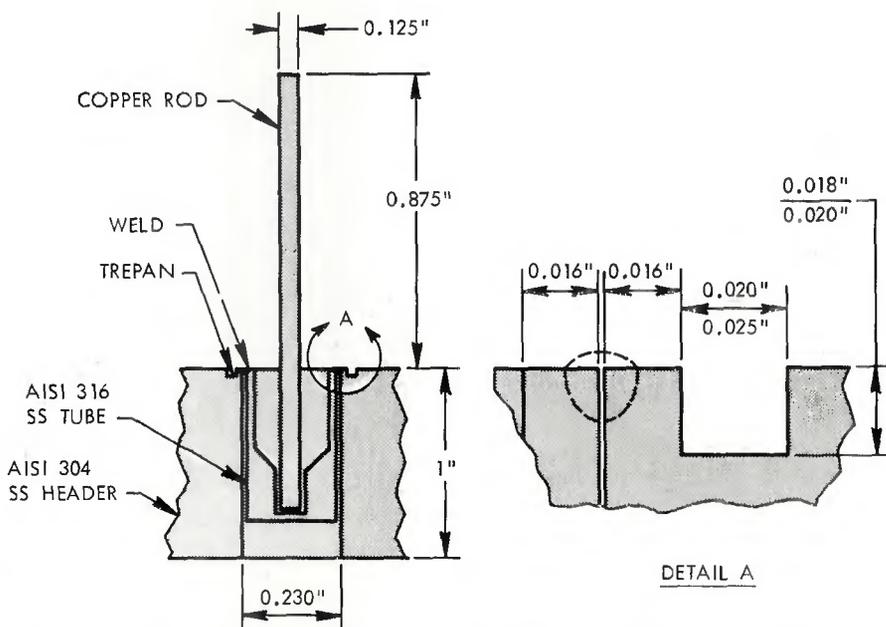

Fig. 7 — Simulated cartridge heater and tube assembly using welding development
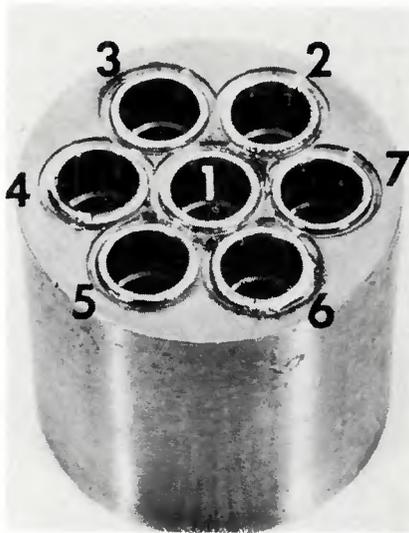
Fig. 8 — A comparison of welds 2 and 5 of Coupon 1 shows the effect of spot weld overlap on bead formation (X4, reduced 55%)
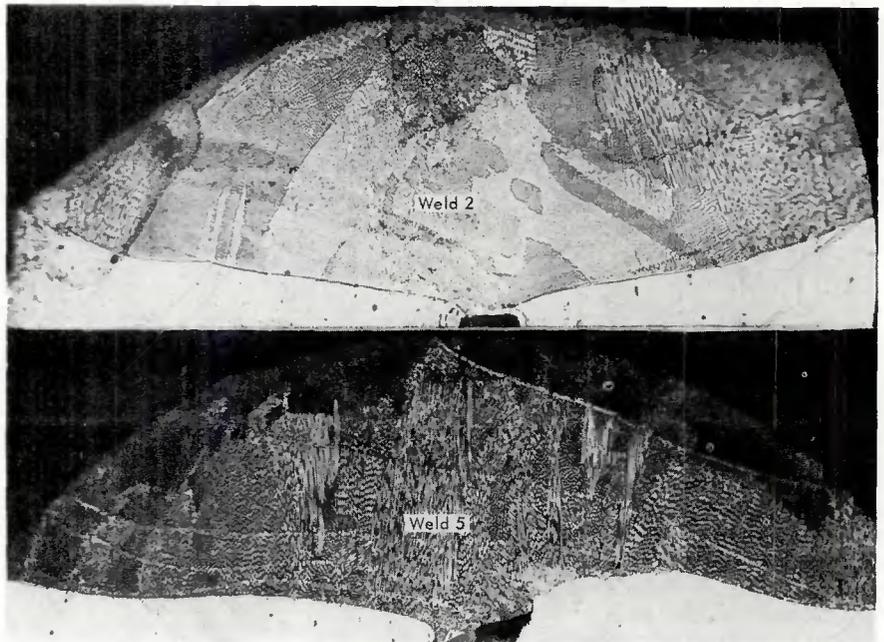

Fig. 9 — Welds 2 and 5 from Coupon 1 (X200, reduced 25%)

same penetration and leak rate for Weld 2 as 4.00 kV and 90% overlap did for Weld 5.

The transverse lines in the fusion zone of Weld 5 are of interest. These lines are traces of interfaces of the overlapping spots and are analagous in origin to the bond line of the weld. The "structure-free" zone is caused by vanishingly slow solidification rates in a rather stagnant zone. The initial increment of solidification of successive spots occurs at a relatively slow rate during the incubation period prior to the onset of cellular growth (Ref. 3).

Another welded coupon is presented in Fig. 10 to illustrate how the close proximity of the rods limits accessibility for welding. Leak rates for these welds were less than 1.0×10^{-9} std cc/sec helium. A force of 530 lb was required to shear the center weld. This test was performed by inverting the coupon and applying a load to a pin in contact with the bottom of the tube which transmitted a shearing force onto the weld.

Prototype Welding and Evaluation

Results on the subsized coupons indicated that further effort was justified; therefore, a full scale prototype of the weld region, including short lengths of heater tubes that were to be used in the mockup, was prepared and welded. This assembly can be seen in the lead photograph.

Laser Beam Geometry

The copper rods of previously welded coupons extended $\sim$ 1.000 in. above the weld surface and had not interfered with the laser beam.

However, the rods in the prototype extended 2.600 in. above the weld and interfered with the beam on the first seven welds. To correct this condition, a test was performed to measure the degree of interference of rods with the beam.

The beam was directed at exposed photographic film placed at various

Fig. 10 — Subsize fuel-failure mockup weld coupon (approx 1.1 in. diam) after welding with copper rods in place

working levels. The cross-sectional image of the beam was recorded at each film position. Then, a precise pattern of the vertical profile of the beam was constructed for the specific spot size setting selected for welding the prototype. Figure 11 shows the relationship between focal distance and the image of the spot diameter. Also, the geometry of the beam used for welding the remainder of the prototype is indicated schematically. The test indicated that a beam with this shape could be used to weld assemblies having copper rods of lengths up to 1.375 in. As a consequence, the copper rods were removed from the prototype and shortened to 1.300 in. and reinserted prior to making the remaining twelve welds.

Weld Procedure

The focal distance was verified by micrometer measurement as previously described. Then, the tube-to-sheet joint was positioned by X-Y adjustments and visually tracked coincident with the reticle of the microscope. Spot welds were made at 90 deg intervals to assure accurate tracking of the joint. The rest of the welding was performed in the automatic mode. The number of spots per joint was deliberately varied from 85 to 125 and five to ten spots were made at reduced energy at the end of each weld to prevent cratering. Spots were approximately 0.030 in. diam, and the overlap of spots ranged from 70 to 95%.

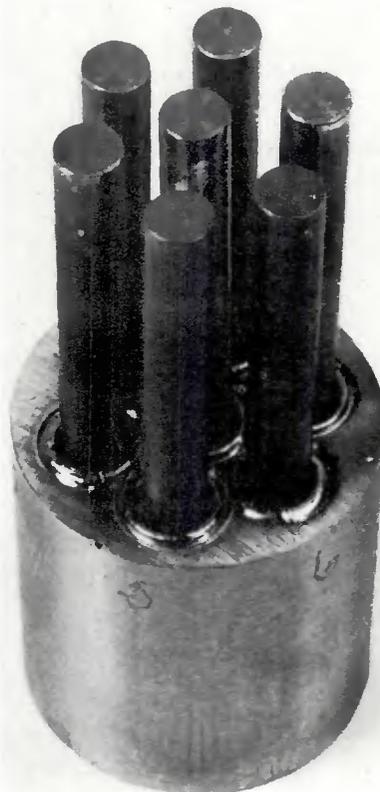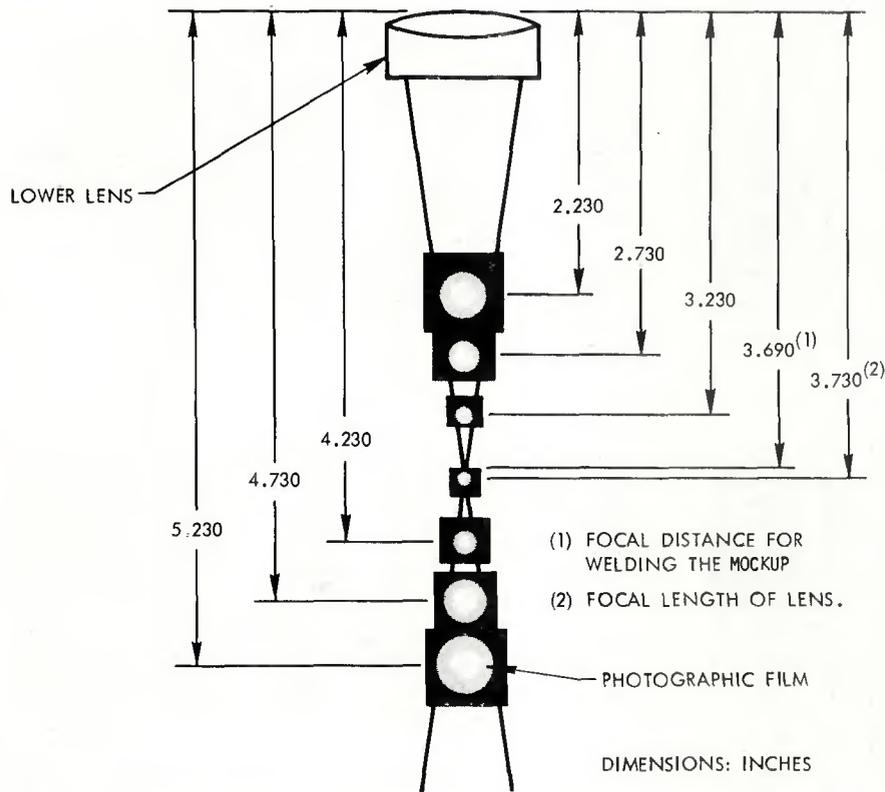The pulse repetition rate was maintained constant at 30 per minute. The welding parameters for these welds

Table 1 — Parameter Variations and Results of Welds in Coupon 1

Weld	Charging voltage, kV	Spot overlap, %	Number of spots	Leak rate std cc/sec He	Penetration, mils
1	4.00	95	125	$< 1.0 \times 10^{-9}$	8-9
2	3.60	50	68	$< 1.0 \times 10^{-9}$	10 - 11
3	3.50	90	105	$< 1.0 \times 10^{-9}$	6 - 7
4	3.20	50	66	3.0×10^{-6}	4 - 5
5	4.00	90	98	$< 1.0 \times 10^{-9}$	9 - 10
6	4.40	90	101	$< 1.0 \times 10^{-9}$	10 - 11
7	3.60	95	120	$< 1.0 \times 10^{-9}$	7 - 8

LOWER LENS

2.230
2.730
3.230
3.690[1]
3.730[2]
4.230
4.730
5.230

(1) FOCAL DISTANCE FOR WELDING THE MOCKUP

(2) FOCAL LENGTH OF LENS.

PHOTOGRAPHIC FILM

DIMENSIONS: INCHES

Fig. 11 — Laser beam geometry determined by beam exposure of photographic film

were varied in accordance with the experience attained in the coupon study. All nineteen welds of the prototype had leak rates less than 1.0×10^{-7} std cc/sec helium except one which was rewelded satisfactorily. The penetrations and cross-sections of four of these welds can be seen in Fig. 12. The parameters for Weld 18, with penetration ranging from 0.015 to 0.020 in. were selected for welding the mockup. The nominal values are listed below:

Charging voltage, kV	4.00
Pulse time, ms	4.5
Cooling water temp., F	60-68
Energy output, Joules	11.5
Spots per weld	101
Focal distance, in.	3.690
Spot Overlap, %	74

Description of Simulated Fuel Subassembly

The laser welding station with simulated fuel subassembly in position

for welding is shown in Fig. 13. The assembly is about 5 ft long with nineteen 0.230 in. diam simulated heater tubes located within a 1.250 in. diam circle. An inverted mirror and lighting arrangement was used to illuminate the area around the tube-to-header joint. This setup provided good visibility for accurately positioning a joint so that it would be tracked by the laser beam. Each joint was aligned under the laser head by the X-Y manually operated positioner located in the lower right corner of the photograph.

Approximately 95 overlapping spot welds were made at the procedure energy setting and four to six spots at decreasing energy inputs to prevent cratering at the completion of the weld. The same parameters were used for making all nineteen welds.

Fifteen of the nineteen welds had unacceptable leak rates because of cracks in the fusion zone of the welds. These results were surprising since weld metal cracking and leak-

ing welds had not been experienced prior to this stage of the program. Post mortem analysis on two of the defective welds revealed a number of conditions that could have caused cracking. Fine particles of copper were found adhering to surfaces adjacent to the weld. Apparently this contamination occurred when the protruding ends of the copper rods were cut off *in situ* to the newly specified length after components were fixed in the assembly. Secondly, the heater tube had been work hardened by the swaging process used in manufacturing the heater-tube assembly. Residual stresses in the unannealed, swaged tube could have caused high strains in the weld metal during the final stage of solidification to aggravate the tendency for hot cracking. Thirdly, fine particles of mica observed adhering on the peripheries of tubes could have become trapped in the joint and ended up in the weld. The source of mica was from the insulation between the copper rods and the AISI 316 tubes.

Metallographic analysis revealed the severity of cracking. Figure 14 shows several fissures in the fusion zone and displacement and hot-tearing at the root of the weld. Cracks tended to extend from stringers in the "dirtier" AISI 316 member of the joint. The microhardness of the swaged tube was 340 DPH compared to 254 DPH for the weld metal. Strain, associated with the thermal relief of residual stresses in the work hardened tube, could have intensified the tearing at the root of the joint as the weld solidified. The weld, base metals, and cracked zones were either scanned or point counted with an electron microprobe analyzer for elements normally present in AISI 316 and 304 stainless steels. It was inferred from these measurements that a deficiency of ferrite in the weld metal could have contributed to hot cracking conditions. Collectively, these findings indicated that more tests would be necessary and that emphasis should be placed on cleanliness and on measures for crack prevention.

Confirmation Tests

Trial welds were made to confirm the cracking that had occurred on the mockup. The joint consisted of AISI 316 stainless steel tubing from the same lot used in the mockup. The header was made to the configuration shown in Fig. 7, but annealed AISI 316 steel was used for the header instead of AISI 304 material. Characteristic x-ray photographs and microprobe scans showed that stringers in the tube material contained up to 12% manganese. Up to 0.6 wt. % carbon was found at local sites in the

weld zone. A probable source of carbon was from graphite electrodes used with the electrical discharge machining process to trepan the header. The same process had been used to trepan the header for the mockup. Measurements with a ferrite indicator showed that weld deposits contained less than 0.5% ferrite.

The micrograph in Fig. 15(a) shows that the cracking tendency still persisted but with less severity. Porosity formed probably when evolving gas from elongated inclusions was trapped in the rapidly solidifying weld metal.

The micrograph in Fig. 15(b) enlarges one of the stringers that intersects the bond line of the weld, and an x-ray photograph of this inclusion, in Fig. 15(c), confirms the high manganese concentration at these sites.

It was concluded that the main cause of cracking was ferrite deficiency in the weld metal.

Ferrite forming elements were introduced into the weld zone by surfacing the AISI 304 header with either ER308 or ER312 filler metal prior to trepanning the joint. The surfaced layer was approximately 1/8 in. thick.

Figure 16 shows a cross-section of

WELD 4

WELD 7

G-419-2-3

G-419-4-5
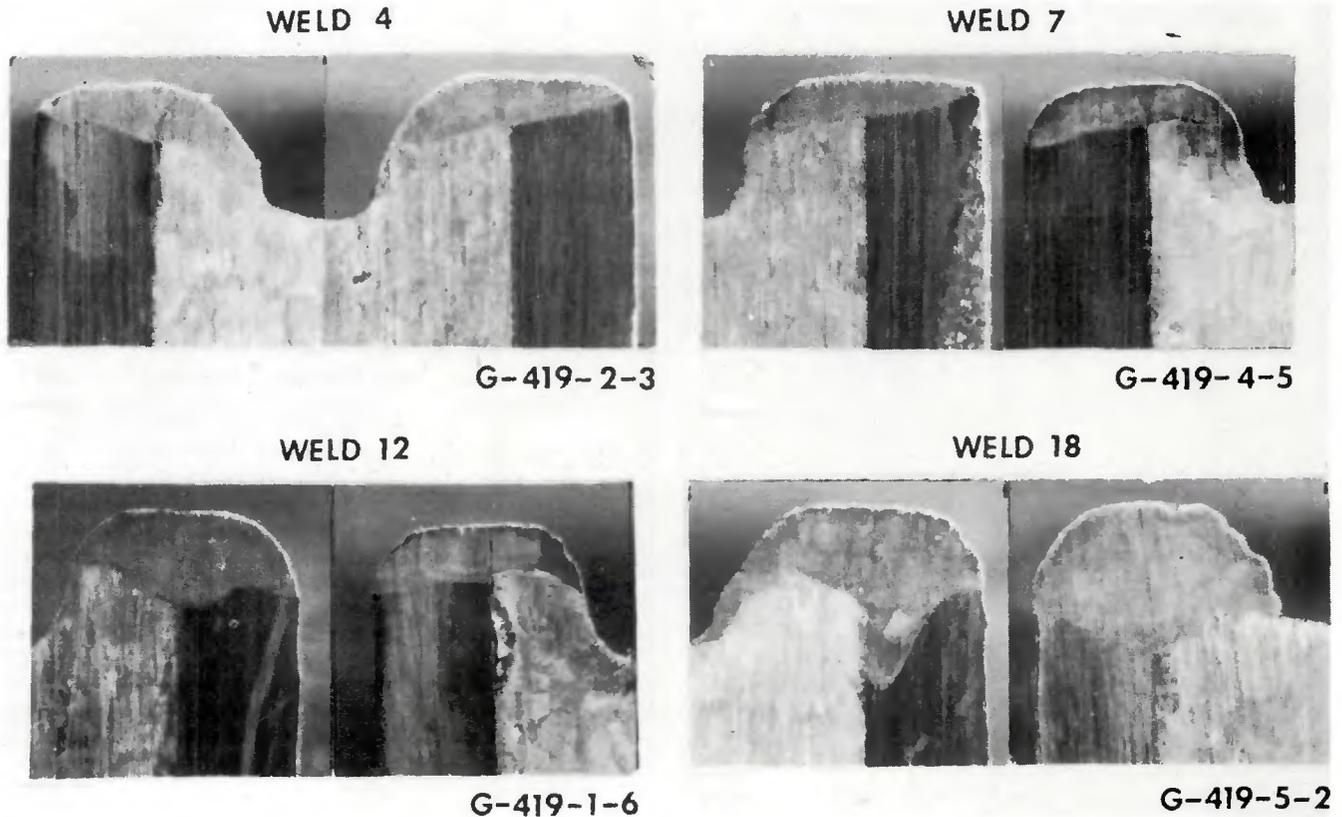
WELD 12

WELD 18

G-419-1-6

G-419-5-2

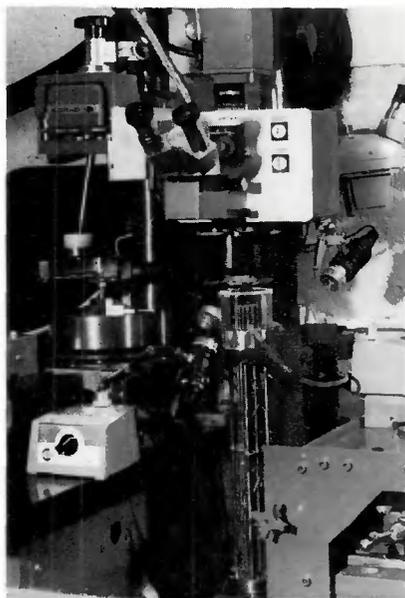Fig. 12 — Welds from prototype 1 made with different parameters (X38)

Fig. 13 — Laser welding station with mockup 1 in position for welding

Fig. 14 — Severe cracking in a laser welded austenitic stainless steel tube-to-header joint (X100, increased 24%)

an experimental laser weld made on the modified joint. The AISI 316 tubing has been annealed. Hardness of the annealed tubing was 151 DPH. The weld deposit hardness was 241 DPH. Annealing has tended to break up the elongated stringers and has relieved residual stresses caused by swaging. The AISI 304 header, surfaced with ER312 filler metal, has enriched the weld metal with ferrite. Satisfactory welds were also made on joints surfaced with ER308 filler metal. A series of welds joining annealed and unannealed tubing to surfaced headers were devoid of fissures; nevertheless, the use of annealed tubing was judged to be the most prudent approach.

Latest Approach

The results of this work have been engineered into fabrication procedures. Headers are being surfaced with ER308 filler metal using the gas tungsten-arc process. After machining, the surfaced layer is about 1/8 in. thick.

The joint grooves are trepanned with the EDM process and subsequently electropolished to remove vestiges of carbon that might have been picked up from the machining electrodes. An annealed, machined AISI 316 adapter is now being gas tungsten-arc welded, using ER308 filler metal, onto the swaged tubes to provide a more weldable combination of materials for the closure joints. This change also made it expedient to relieve the mica from the vicinity of the weld and significantly improved the ability to keep the joint clean. The minimum joint strength, in terms of weld penetration, has been changed from 0.012 to 0.016 in. (i.e., from 3/4 to 1 times the wall thickness of the tubing) to increase joint efficiency.

Provisions were made to use electron beam welding for these fuel bundles since the laser used in the present work was not suitable for making welds ranging above 0.016 in. in penetration. Also, an electron-beam welding procedure for a similar joint had been developed at another AEC laboratory. Typical parameters now being used by a commercial
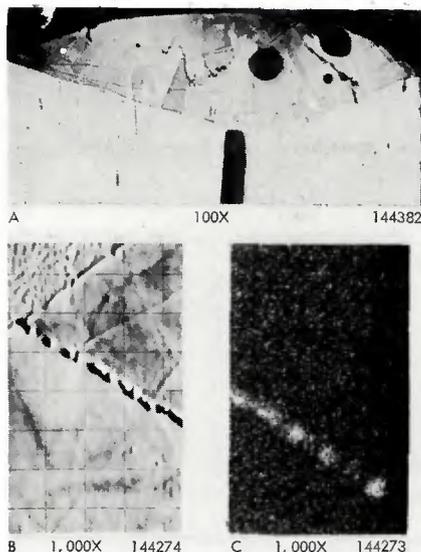

Fig. 15 — Evaluation of post mockup test weld in AISI 316 stainless steel showing (a) fissures and porosity in the weld metal, (b) enlarged view of largest stringer in left (tube) member, and (c) an x-ray photograph of the area indicating presence of manganese (all reduced 48%)

Fig. 16 — Laser weld joining an annealed mockup heater tube (left side) to AISI 304 stainless steel surfaced with ER312 filler metal (X100, reduced 25%)

fabricator are 70 kV, 1.5 mA, 20 rpm, and a minimum (sharp) beam focus at the joint surface. The joints of the assembly are positioned in succession with the beam by an eccentric table that rotates under a fixed Steigerwald Type S-32 gun. The welding current is preset to decay gradually in terminating the weld. The process has performed satisfactorily, and three assemblies have been fabricated to date with this electron beam procedure.

References

1. Moorhead, A. J. and Turner, P. W., "Welding a Thermocouple Gauge to Apollo Lunar Sample Return Containers," *Welding Journal,* 49 (1), pp. 15-21, January, 1970.
2. Turner, P. C., Unpublished Work, Union Carbide Corporation, Nuclear Division, Y-12 Plant, Oak Ridge, Tennessee.
3. Tiller, W. A., Jackson, K. A., Rutter, J. W., and Chalmers, B., *Acta Met.,* 1, 428 (1953).

Bibliography

1. "Laser Welding and Machining," *Engineering Proceedings P-44,* Fifteen Papers Presented at the Engineering Seminar on New Industrial Technologies at the Pennsylvania State University, June 27-July 2, 1965.
2. Anderson, J. E., and Jackson, J. E., "Theory and Application of Pulsed Laser Welding," *Welding Journal,* 44 (12), pp. 1018-1026; December, 1965.
3. Earvolino, L. P., and Kennedy, J. R., "Laser Welding of Aerospace Structural Alloys," *Welding Journal,* 45 (3), Research Suppl., pp. 127-s to 134-s, March, 1966.
4. "Laser Beam Welding," *Welding Handbook,* Sixth Edition, Section 3B, 55.1-55.20, 1971.
5. Cohen, M. I., Melone, T. G., and Mainwaring, F. J., "Laser Interconnection of Wires," *Welding Journal,* 48 (3), pp. 191-197, March, 1969.
6. Fairbanks, R. H., Sr., and Adams, C. M., Jr., "Laser Beam Fusion Welding," *Welding Journal,* 43 (3), Research Suppl., pp. 97-s to 102-s, March, 1964.

WELDING METALLURGY | *Concisely presented information of great value to everyone in the industry*

WELDING METALLURGY, by George E. Linnert, offers a concise but comprehensive treatment of the great mass of technical information now available in this field. The subject matter is divided into two volumes.

Volume I — Fundamentals — is designed to provide the basic information necessary for any real understanding of welding as a major tool of the steel fabricating industry. It begins with the essentials of welding and metallurgy, considered separately. It concludes with a study showing how the welding thermal cycle alters the microstructure of the joint and how this alteration, in turn, affects joint properties.

In Volume II — Technology — the earlier material is developed in greater detail, focusing on the specific factors and conditions that require consideration when dealing with particular projects. The discussions, illustrations, and data tables in Volume 2 again follow the basic metallurgical approach to each subject area. In this manner, a strong understanding of the basics is provided, which the reader may easily reinforce by specialized study into whatever other aspects are deemed important.

These two volumes will prove useful not only in orienting the novice welding engineer to this broad field of welding, but also in helping the more experienced professional who needs assistance in finding a rational basis for solving problems.

<div align="center">

Volume I, Fundamentals $12.00
Volume II, Technology $14.00

</div>

Discounts: 25% to A and B members; 20% to bookstores, public libraries and schools; 15% to C and D members.

Send your order to the American Welding Society, 2501 NW 7th St., Miami, FL 33125. Florida residents add 4% sales tax.

WELDING INSPECTION | *An introduction to the subject that even experienced inspectors will refer to often*

WELDING INSPECTION describes the general duties and responsibilities of inspectors of weldments. Because the discussions are more general than those found in particular codes and specifications, it is especially useful for training inspectors.

Among the topics covered are: requirements for an inspector; duties of an inspector; welding procedure specification; qualification of welding procedures; qualification of welders and welding operators; weldment defects, and destructive and nondestructive testing of welds. $9.00.

Discounts: 25% to A and B members; 20% to bookstores, public libraries and schools; 15% to C and D members.

Send your order to the American Welding Society, 2501 NW 7th St., Miami, FL 33125. Florida residents add 4% sales tax.